Original Article | Gastrointestinal Imaging

eISSN 2005-8330
https://doi.org/10.3348/kjr.2023.0295
Korean J Radiol 2024;25(3):243-256

Korean Journal of Radiology
KJR

Evaluation of Malignancy Risk of Ampullary Tumors Detected by Endoscopy Using 2-[^{18}F]FDG PET/CT

Pei-Ju Chuang[1], Hsiu-Po Wang[2], Yu-Wen Tien[3], Wei-Shan Chin[4], Min-Shu Hsieh[5], Chieh-Chang Chen[2], Tzu-Chan Hong[2,6], Chi-Lun Ko[7], Yen-Wen Wu[8,9], Mei-Fang Cheng[7,10]

[1]Department of Nuclear Medicine, National Taiwan University Hospital, Yunlin Branch, Yunlin, Taiwan
[2]Department of Internal Medicine, National Taiwan University Hospital, National Taiwan University College of Medicine, Taipei, Taiwan
[3]Department of Surgery, National Taiwan University Hospital, National Taiwan University College of Medicine, Taipei, Taiwan
[4]School of Nursing, National Taiwan University College of Medicine, Taipei, Taiwan
[5]Department of Pathology, National Taiwan University Hospital, National Taiwan University College of Medicine, Taipei, Taiwan
[6]Department of Internal Medicine, National Taiwan University Cancer Centre, Taipei, Taiwan
[7]Department of Nuclear Medicine, National Taiwan University Hospital, National Taiwan University College of Medicine, Taipei, Taiwan
[8]School of Medicine, College of Medicine, National Yang Ming Chiao Tung University, Taipei, Taiwan
[9]Department of Nuclear Medicine and Cardiovascular Medical Centre (Cardiology), Far Eastern Memorial Hospital, New Taipei City, Taiwan
[10]Institute of Environmental and Occupational Health Sciences, National Taiwan University, Taipei, Taiwan

Objective: We aimed to investigate whether 2-[^{18}F]fluoro-2-deoxy-D-glucose positron emission tomography/computed tomography (2-[^{18}F]FDG PET/CT) can aid in evaluating the risk of malignancy in ampullary tumors detected by endoscopy.

Materials and Methods: This single-center retrospective cohort study analyzed 155 patients (79 male, 76 female; mean age, 65.7 ± 12.7 years) receiving 2-[^{18}F]FDG PET/CT for endoscopy-detected ampullary tumors 5–87 days (median, 7 days) after the diagnostic endoscopy between June 2007 and December 2020. The final diagnosis was made based on histopathological findings. The PET imaging parameters were compared with clinical data and endoscopic features. A model to predict the risk of malignancy, based on PET, endoscopy, and clinical findings, was generated and validated using multivariable logistic regression analysis and an additional bootstrapping method. The final model was compared with standard endoscopy for the diagnosis of ampullary cancer using the DeLong test.

Results: The mean tumor size was 17.1 ± 7.7 mm. Sixty-four (41.3%) tumors were benign, and 91 (58.7%) were malignant. Univariable analysis found that ampullary neoplasms with a blood-pool corrected peak standardized uptake value in early-phase scan (SUVe) ≥ 1.7 were more likely to be malignant (odds ratio [OR], 16.06; 95% confidence interval [CI], 7.13–36.18; P < 0.001). Multivariable analysis identified the presence of jaundice (adjusted OR [aOR], 4.89; 95% CI, 1.80–13.33; P = 0.002), malignant traits in endoscopy (aOR, 6.80; 95% CI, 2.41–19.20; P < 0.001), SUVe ≥ 1.7 in PET (aOR, 5.43; 95% CI, 2.00–14.72; P < 0.001), and PET-detected nodal disease (aOR, 5.03; 95% CI, 1.16–21.86; P = 0.041) as independent predictors of malignancy. The model combining these four factors predicted ampullary cancers better than endoscopic diagnosis alone (area under the curve [AUC] and 95% CI: 0.925 [0.874–0.956] vs. 0.815 [0.732–0.873], P < 0.001). The model demonstrated an AUC of 0.921 (95% CI, 0.816–0.967) in candidates for endoscopic papillectomy.

Conclusion: Adding 2-[^{18}F]FDG PET/CT to endoscopy can improve the diagnosis of ampullary cancer and may help refine therapeutic decision-making, particularly when contemplating endoscopic papillectomy.

Keywords: Ampulla of Vater; Endoscopy; 2-[^{18}F]fluoro-2-deoxy-D-glucose; Positron emission tomography; Risk assessment

INTRODUCTION

All ampullary neoplasms need to be excised because of their potential for malignant transformation [1-5]. Being less invasive and equally effective in removing the tumors [3-10], endoscopic papillectomy (EP) has been proposed

Received: March 31, 2023 **Revised:** December 8, 2023 **Accepted:** December 31, 2023
Corresponding author: Mei-Fang Cheng, MD, PhD, Department of Nuclear Medicine, National Taiwan University Hospital, National Taiwan University College of Medicine, No. 7, Chung-Shan South Road, Chung-Cheng District, Taipei 100, Taiwan
• E-mail: meifang@ntuh.gov.tw

as a suitable alternative to pancreaticoduodenectomy in treating benign adenomas [1,3-12]. Nonetheless, the lack of a thorough nodal survey may have led to underestimation of the disease stage and subsequent inadequate treatment [3-6]. Histopathology of biopsy specimens is considered a reliable method to identify malignancy [3]; however, concordance rates of only 40%–70% have been reported for biopsy and surgically resected specimens [4]. Moreover, 15%–60% of presumed benign adenomas have been found to harbor small foci of adenocarcinoma after resection [3-5,7,8,12].

The European Society of Gastrointestinal Endoscopy supports the use of endoscopic ultrasonography (EUS) and magnetic resonance cholangiopancreatography (MRCP) for the preoperative staging of ampullary tumors [3]. EUS provides accurate T staging [3-5,7,8]. Despite the modest sensitivity of contrast-enhanced computed tomography (CT) in detecting malignant ampullary neoplasms, abrupt narrowing of the distal common bile duct and intrahepatic ductal dilatation are important signs for diagnosing malignancies [13,14]. Better N staging performance has been reported using MRCP than using EUS or contrast-enhanced CT; however, these studies only included a limited number of patients [3,15].

2-[^{18}F]fluoro-2-deoxy-D-glucose positron emission tomography/CT (2-[^{18}F]FDG PET/CT) can image tumors with increased glycolysis [16], especially highly mitotic cells with KRAS mutations and Ki-67 overexpression [17-19]. These immunohistopathologic characteristics are also frequently seen in ampullary cancer [1,20-22]. Previous studies reported that 2-[^{18}F]FDG PET/CT can help evaluate tumor invasion and predict survival in ampullary cancer [23-25]. In this study, we aimed to investigate whether 2-[^{18}F]FDG PET/CT could help evaluate the risk of malignancy in endoscopy-detected ampullary tumors.

MATERIALS AND METHODS

Patients

This study was approved by the Institutional Review Board of the National Taiwan University Hospital (NTUH-IRB No. 202309007RINA). This retrospective study analyzed patients from a prospectively established observational cohort at the PET center of a university hospital in Northern Taiwan. From June 2007 to December 2020, consecutive patients referred by gastroenterologists for PET/CT of endoscopy-

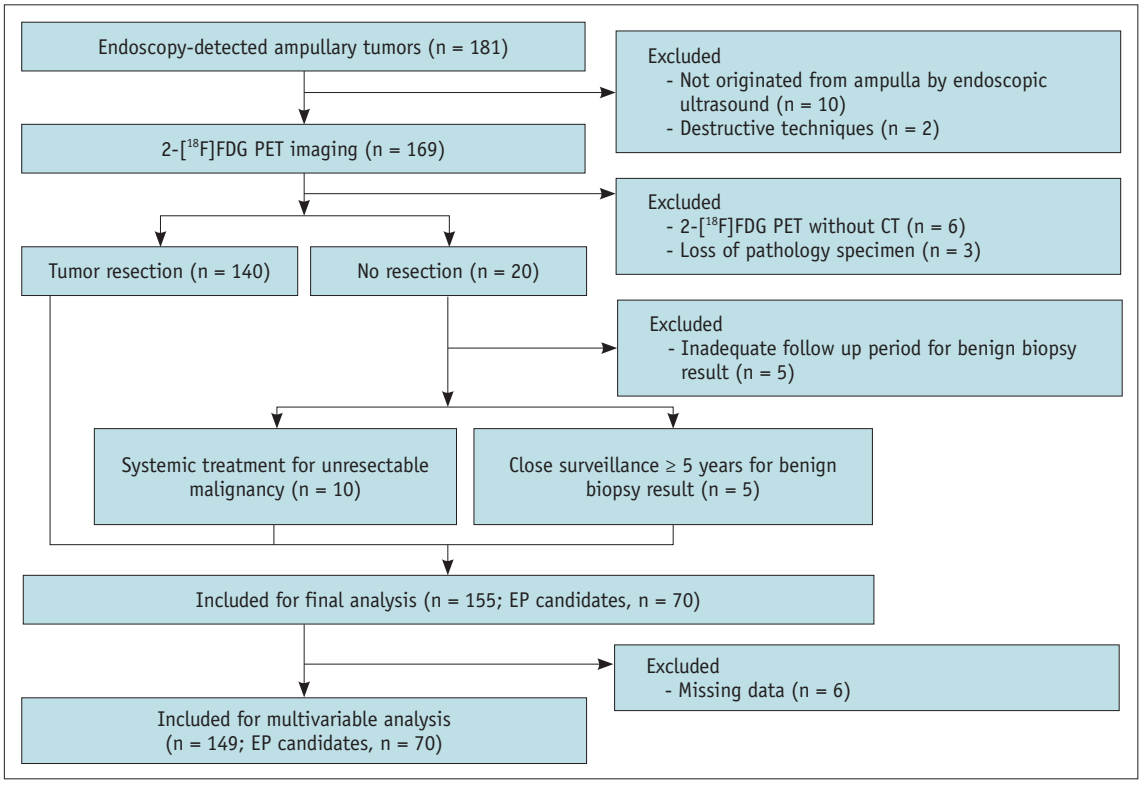

Fig. 1. Flow diagram of study participants. 2-[^{18}F]FDG PET = 2-[^{18}F]fluoro-2-deoxy-D-glucose positron emission tomography, CT = computed tomography, EP = endoscopic papillectomy

https://doi.org/10.3348/kjr.2023.0295

Korean Journal of Radiology
KJR

detected ampullary tumors were prospectively enrolled [23]. 2-[18F]FDG PET/CT was performed 5–87 days (median of 7 days) after diagnostic endoscopy to avoid procedure-related inflammation. Only patients who underwent tumor resection or active endoscopic surveillance for ≥ 5 years were included in this analysis (Fig. 1). The details are shown in Figure 1. All participants signed an informed consent form before undergoing PET/CT imaging.

Clinical Data Collection and Diagnostic Endoscopy

Clinical information, including presenting symptoms and signs, and serum tumor marker (carbohydrate antigen 19-9 [CA19-9] and carcinoembryonic antigen) levels, was collected for analysis. The presence of malignant traits on the initial diagnostic endoscopy, including ulceration, spontaneous bleeding, friability, or submucosal involvement [12], and other endoscopic parameters, such as tumor size and the presence of ductal dilatation, were also recorded for analysis. Additional EUS or endoscopic retrospective cholangiopancreatography was performed to clarify tumor depth or ductal invasion whenever the gastroenterologists considered it necessary [4].

PET Imaging Protocol and Interpretation

All patients with a serum glucose level < 150 mg/dL, after a 6-hour fasting period, received 5–6 MBq/kg of 2-[18F]FDG intravenously. PET images were collected using PET/CT scanners routinely used at the NTUH PET Center (Discovery LS or Discovery 710, GE Medical Systems, Milwaukee, WI, USA). Following institutional and international guidelines [26], images were acquired 60 min post-injection (early-phase) from the mid-thigh to the head in 2D or 3D mode with 3-minute bed positions [23,27]. Before the delayed-phase scan (2-hour post-injection), bowel loop distention was achieved using an oral foaming contrast agent (Tae Joon Top Effervescent G Granule, Tae Joon Pharm, Seoul, South Korea). The PET images were iteratively reconstructed using the Ordered Subset Expectation Maximization algorithm with low-dose CT for attenuation correction and anatomical alignment. Calibration of each PET scanner was achieved using a National Electrical Manufacturers Association (NEMA) Image Quality (IQ) phantom, thereby standardizing standardized uptake values (SUVs) and aligning contrast recovery and reconstructions [28,29].

Two board-certified nuclear medicine specialists, each with more than 15 years of PET/CT experience, independently analyzed the anonymized early- and delayed-phase images using the Xeleris (GE Medical Systems) or Syngo.via (Siemens Healthcare, Knoxville, TN, USA) software. Each ampullary lesion's uptake intensity and morphology were visually rated on a 5-point scale in relation to the normal liver [30] (Fig. 2): 1) definitively malignant (intense, focal uptake exceeding liver), 2) likely malignant (moderate, focal uptake exceeding liver), 3) equivocal (mild, focal uptake equal to or slightly greater than liver), 4) likely benign (uptake equal to liver, not focal), and 5) definitively benign (uptake less than liver, linear-like). A consensus malignancy score of ≤ 2 was agreed upon by both readers after discussion. Likewise, lymph node involvement was identified through the evaluation of morphology and intensity uptake exceeding background activity, unrelated to normal structures or artifacts. Semi-quantitation of SUVs (tissue concentration x injection dose^{-1} x body weight) of the main lesion was calculated on attenuation-corrected images using built-in software [16] and corrected with background blood-pool activity. Background blood pool activity was determined as the mean SUV (SUVmean) of a 1 cm diameter and 2 cm height columnar volume of interest placed within the descending aorta. The corrected peak SUV (SUVpeak) of the lesion was calculated from the tumor-to-blood-pool ratio for both early- (SUVe) and delayed-phase (SUVd) scans. Thus, the retention index (RI, [SUVd - SUVe] / SUVe x 100%) of the ampullary lesion was obtained [31,32]. Tumor volume was autosegmented at 40% of the maximum SUV (SUVmax), with manual corrections made in reference to low-dose CT to exclude physiological bowel or renal activity when needed [17,31]. Total lesion glycolysis (TLG, segmented tumor volume x SUVmean) was also calculated to represent the degree of upregulated glycolytic activity [17].

Patient Management

Decisions on resectability, including EP (ampullary tumor ≤ 30 mm in diameter and without evidence of intraductal growth in endoscopy [1,3,5-7]), were made in multidisciplinary discussions involving gastroenterologists, oncologists, radiologists, and nuclear medicine physicians. The resection method was decided based on all available information, including endoscopy, PET/CT, and the patient's consent.

Standard of Reference

The reference standard was defined based on histopathology. Any malignant component revealed on biopsy or resected specimens was categorized as malignant

 https://doi.org/10.3348/kjr.2023.0295

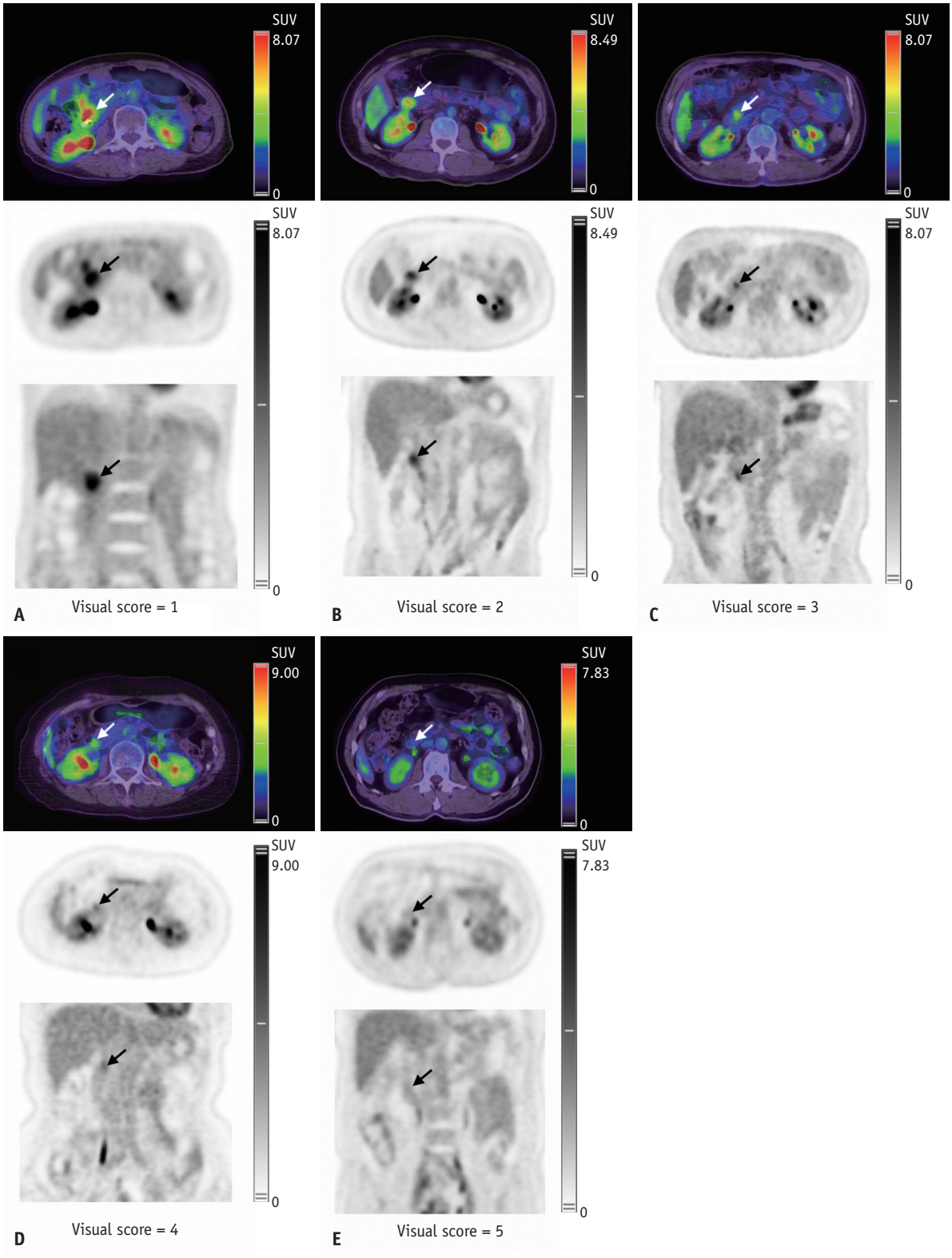

Fig. 2. Demonstration of the positron emission tomography 5-point scale in the visual assessment of each ampullary lesions (arrows) in axial and coronal views. **A:** A definitively malignant lesion with focal and intense uptake greater than liver was graded with a visual score of 1. **B:** A likely malignant lesion with focal uptake greater than liver was graded with a visual score of 2. **C:** An equivocal lesion with mild, but focal uptake equal to or slightly greater than liver, was graded with a visual score of 3. **D:** A likely benign lesion with uptake equal to liver without focal activity was graded with a visual score of 4. **E:** A definitively benign lesion with uptake less than liver was graded with a visual score of 5. SUV = standardized uptake value

https://doi.org/10.3348/kjr.2023.0295

Korean Journal of Radiology
KJR

disease. Any suspicious lymph nodes or distant metastases revealed by conventional imaging or PET/CT were histopathologically confirmed. A specimen classified as benign after curative resection or a benign biopsy followed by ≥ 5 years of negative endoscopic surveillance was categorized as benign disease.

Follow-Up and Surveillance

Patients undergoing tumor resection undergo biannual serum tumor marker checks and imaging, whereas those undergoing only endoscopic procedures undergo additional surveillance within 6 months, followed by a 3–12-month interval follow-up [4]. Biopsies were performed for suspected recurrence on endoscopy.

Statistical Analysis

Data were presented as number (%) and mean ± standard deviation (SD), or median with interquartile range (IQR) if significant skewness was observed. Factors were compared between the benign and malignant groups using *t*-test for parametric data and Wilcoxon-Mann-Whitney U test for nonparametric data. Visual assessment of the PET images was correlated with the final diagnosis using the chi-square test, and interobserver agreement was calculated using Cohen's kappa test. Semiquantitative PET parameters were analyzed using receiver operating characteristic (ROC) curves, with optimal cut-off values determined using the Youden method [33]. The performance of standard endoscopy and PET parameters for diagnosing malignancy was compared. The risk factors for malignancy were examined for their ability to distinguish malignant from benign neoplasms by comparing one parameter with the outcome (cancer or not) at a time. Parameters showing a significant relationship ($P < 0.05$) were included in the multivariable analysis. Patients with missing data were excluded from the multivariable analysis. Multivariable logistic regression analysis with backward stepwise factor selection was used to achieve the best value for the Akaike information criterion and an additional bootstrapping method. A risk model combining PET findings with clinical and endoscopic findings was developed using the significant parameters derived from multivariable logistic regression analysis of the entire cohort. The performance of the model, including the area under the curve (AUC) and diagnostic performance at the optimal cut-off value determined using the Youden method, was compared with that of endoscopic diagnosis with or without clinical findings using the DeLong test. The same risk model and cut-off value were further applied to a subgroup of patients selected as EP candidates by endoscopy criteria, i.e. those with an ampullary tumor ≤ 30 mm and without intraductal growth. A *P*-value < 0.05 was considered statistically significant. All data were analyzed using SPSS version 26.0 (IBM Corp., Armonk, NY, USA).

RESULTS

Patient Characteristics

A total of 155 patients (79 male and 76 female; mean age, 65.7 ± 12.7 years) were analyzed (Table 1). Among these, 70 (45.2%) patients were candidates for EP according to international guidelines [3,4]. The baseline characteristics of the included patients are presented in Table 1. The prevalence of jaundice and fever was higher in the malignant lesion group, whereas more patients with benign lesions experienced abdominal pain (Table 1). Other clinical factors did not differ significantly between the groups. More patients had elevated CA19-9 levels in the malignant group (48.4% [44/91]) than in the benign group; however, the difference in the elevated levels was not significant ($P = 0.068$; Table 1). Additionally, there was no significant difference in the time interval between the endoscopic biopsy and PET between the benign and malignant groups ($P = 0.196$).

The median time interval between PET/CT and pathological confirmation was 8 days (IQR, 2–25 days) in the entire cohort. Ninety-one patients (58.7%) underwent surgical resection, 49 (31.6%) underwent EP, 5 (3.2%) underwent active endoscopic surveillance, and 10 (6.5%) received chemotherapy alone (M1 disease) (Table 1). The mean tumor size, measured by endoscopy, was 17.1 ± 7.7 mm. Twenty-one (23.1%) ampullary cancers were identified as non-dysplastic or low-grade dysplastic neoplasms by biopsy, and 19/29 (65.5%) high-grade dysplastic biopsy specimens were later proven to harbor invasive components. Thirty-five (38.5%) of the 91 patients who underwent surgery were diagnosed with N1 disease, and distant metastases were found in 10 (11.0%) of the entire cohort. Details of the other histopathological findings are listed in Supplementary Table 1.

Endoscopic Features and PET Parameters

Malignant tumors were more likely to exhibit malignant traits in endoscopy (81.3% [74/91] vs. 32.8% [21/64], $P < 0.001$), cause biliary or pancreatic duct dilatation (88.1% [74/84] vs. 63.5% [40/63], $P < 0.001$), and were

 https://doi.org/10.3348/kjr.2023.0295

Table 1. Patient characteristics and comparisons of different pathology groups

	All (n = 155)	Pathology groups		*P*
		Benign (n = 64)	Malignant (n = 91)	
Age, yrs	65.7 ± 12.7	66.9 ± 11.7	64.9 ± 13.3	0.433
Sex, male	79 (51.0)	33 (51.6)	46 (50.6)	0.903
BMI, kg/m^2	24.0 ± 3.9	24.3 ± 3.9	23.7 ± 4.0	0.211
Diabetes	43 (27.7)	17 (26.6)	26 (28.6)	0.786
Dyslipidemia	20 (12.9)	11 (17.2)	9 (9.9)	0.185
Smoking	42 (30.4)	15 (25.9)	27 (33.8)	0.323
Drinking	24 (17.4)	10 (17.2)	14 (17.5)	0.971
Presenting symptoms				
Pain	64 (41.3)	36 (56.3)	28 (30.8)	0.002
Jaundice	63 (40.7)	10 (15.6)	53 (58.2)	< 0.001
Fever	27 (17.4)	6 (9.4)	21 (23.1)	0.027
CA19-9				
Elevated (≥ 37 U/mL)	56 (36.1)	12 (18.8)	44 (48.4)	< 0.001
Level*, U/mL	145.1 (50.7–1226.5)	53.1 (42.5–222.2)	160.2 (57.0–1391.0)	0.068
CEA				
Elevated (≥ 5 ng/mL)	14 (9.0)	3 (4.7)	11 (12.1)	0.115
Level*, U/mL	10.7 (5.9–20.6)	7.4 (5.1–23.4)	11.3 (6.1–20.3)	0.586
Endoscopic procedure before PET				
Biopsy before PET				
Patients	138 (89.0)	57 (89.1)	81 (89.0)	
Time until PET, days	8.0 (5.0–15.0)	10.5 (5.0–21.3)	8.0 (5.0–17.8)	
Drainage before PET				
Patients	75 (48.4)	26 (40.6)	49 (53.8)	
Time until PET, days	9.0 (6.0–19.0)	16.5 (7.0–44.3)	8.0 (5.0–18.0)	
Patient management				
Surgical resection†	91 (58.7)	15 (23.4)	76 (83.5)	
Endoscopic papillectomy	49 (31.6)	44 (68.8)	5 (5.5)	
Observational surveillance	5 (3.2)	5 (7.8)	0 (0)	
Chemotherapy alone	10 (6.5)	0 (0)	10 (11.0)	

Data are mean ± standard deviation, median (interquartile range), or number of patients (%).
*Tumor marker distribution only demonstrated in patients with elevated levels, †Surgical resection includes Whipple's procedure, pyloric preserving pancreaticoduodenectomy, and local resection.
BMI = body mass index, CA19-9 = carbohydrate antigen 19-9, CEA = carcinoembryonic antigen, PET = positron emission tomography

larger in size (19.2 ± 8.4 mm vs. 14.6 ± 5.9 mm, *P* = 0.003, Table 2). Good sensitivity (81.3%; 95% confidence interval [CI], 72.1%–88.0%) but lower specificity (67.2%; 95% CI, 55.0%–77.4%) was observed using endoscopically detected malignant traits to differentiate cancer from benign tumors (Table 3). Malignant tumors demonstrated a sensitivity of 61.5% (95% CI, 50.8%–71.6%) and specificity of 87.5% (95% CI, 76.9%–94.5%) in early-phase PET images and 65.9% (95% CI, 55.3%–75.6%) and 89.1% (95% CI, 78.8%–95.5%) in delayed-phase images. Interobserver agreement was superior in delayed-phase scans over early-phase, with κ values increasing from 0.71 to 0.88. The semiquantitative PET parameters of the primary tumor also differed significantly between the two groups (*P* < 0.001; Table 2, Fig. 3). Youden's method proposed an SUVe cut-off of 1.7 to detect malignancy, offering a sensitivity of 76.9% (95% CI, 67.3%–84.4%), specificity of 82.8% (95% CI, 71.8%–90.1%), and accuracy of 79.4% (95% CI, 72.1%–85.4%) (Table 3). With an RI cut-off of 35%, the sensitivity, specificity, and accuracy were 78.9% (95% CI, 69.0%–86.8%), 56.3% (95% CI, 43.3%–68.6%), and 69.5% (95% CI, 61.6%–76.6%), respectively. Using a TLG cut-off of 7.0, the sensitivity, specificity, and accuracy were 77.8% (95% CI, 67.8%–85.9%), 73.4% (95% CI, 60.9%–83.7%), and 76.0% (95% CI, 68.4%–82.5%), respectively.

In 64 patients with benign tumors, only 3 (4.7%) had

https://doi.org/10.3348/kjr.2023.0295

Korean Journal of Radiology
KJR

Table 2. Endoscopy and PET findings of the different pathology groups

	All (n = 155)	Pathology groups		*P*
		Benign (n = 64)	Malignant (n = 91)	
Endoscopy findings				
Malignant traits	95 (61.3)	21 (32.8)	74 (81.3)	< 0.001
Size, mm	17.1 ± 7.7	14.6 ± 5.9	19.2 ± 8.4	0.003
Ductal dilatation	114 (77.6)	40 (63.5)	74 (88.1)	< 0.001
Biliary duct dilatation	95 (64.6)	27 (42.9)	68 (81.0)	< 0.001
Pancreatic duct dilatation	79 (53.7)	29 (46.0)	50 (59.5)	0.106
PET findings				
Ampullary tumor				
Positive visual assessment				
Early-phase	64 (41.3)	8 (12.5)	56 (61.5)	< 0.001
Delayed-phase	67 (43.5)	7 (11.0)	60 (66.7)	< 0.001
Semiquantitation				
SUVe	1.7 (1.2–3.0)	1.3 (1.0–1.6)	2.5 (1.7–3.7)	< 0.001
RI, %	47.5 (27.0–72.0)	30.5 (16.3–59.5)	58.5 (37.0–75.3)	< 0.001
TLG	7.7 (4.3–21.1)	4.9 (2.8–7.0)	13.9 (7.3–37.4)	< 0.001
Positive node	41 (26.5)	3 (4.7)	38 (41.8)	< 0.001
Metastasis	9 (5.8)	0 (0.0)	9 (9.9)	0.010

Data are mean ± standard deviation, median (interquartile range), or number of patients (%).
PET = positron emission tomography, SUVe = blood-pool corrected peak standardized uptake value in early-phase scan, RI = retention index, TLG = total lesion glycolysis

Table 3. Diagnostic performance of endoscopy and PET

	Endoscopy	PET (SUVe ≥ 1.7)	*P*
Sensitivity	81.3 (74/91) [72.1-88.0]	76.9 (70/91) [67.3-84.4]	0.466
Specificity	67.2 (43/64) [55.0-77.4]	82.8 (53/64) [71.8-90.1]	0.041
Accuracy	75.5 (117/155) [67.9-82.0]	79.4 (123/155) [72.1-85.4]	0.561
Positive predictive value	77.9 (74/95) [68.6-85.1]	86.4 (70/81) [77.3-92.2]	0.144
Negative predictive value	71.7 (43/60) [59.2-81.5]	71.6 (53/74) [60.0-80.6]	0.995

Data are percentages with raw numbers in parentheses and 95% confidence interval values in brackets.
PET = positron emission tomography, SUVe = blood-pool corrected peak standardized uptake value in early-phase scan

false-positive nodes on PET, but no false-positive metastasis was found (Table 2). A PET-positive node suggested malignancy with 95.3% specificity (95% CI, 86.9%–99.0%) and 92.7% (95% CI, 80.1%–98.5%) positive predictive value (PPV), while PET-positive distant metastasis displayed both 100% specificity (95% CI, 94.4%–100%) and PPV (95% CI, 66.4%–100%). Among 76 cancer patients undergoing surgery, PET/CT showed a 54.3% (95% CI, 36.7%–71.2%) sensitivity for detecting nodal metastases.

Risk Factors and Prediction Model for Ampullary Cancer

Univariable analysis revealed that the absence of pain, jaundice, fever, elevated serum CA19-9 levels, and endoscopic features were significantly associated with malignancy (Table 4). All PET-derived parameters, notably ampullary tumors with SUVe ≥ 1.7 (odds ratio [OR], 16.06, $P < 0.001$), and PET-positive nodes were significant malignancy predictors (Table 4). Similar findings were observed for the EP candidates (Supplementary Table 2).

A total of 149 patients were included in the multivariable analysis, after excluding 6 patients with missing data (Fig. 1). After backward stepwise variable selection, multivariable regression analysis identified jaundice, malignant traits in endoscopy, a hypermetabolic ampullary tumor with SUVe ≥ 1.7, and PET-positive node as independent predictors of malignancy (Table 4). The risk model, which was developed using these significant parameters, was further validated using the bootstrapping method with 997 resampling times. This validation process generated similar coefficients and yielded comparable model

 https://doi.org/10.3348/kjr.2023.0295

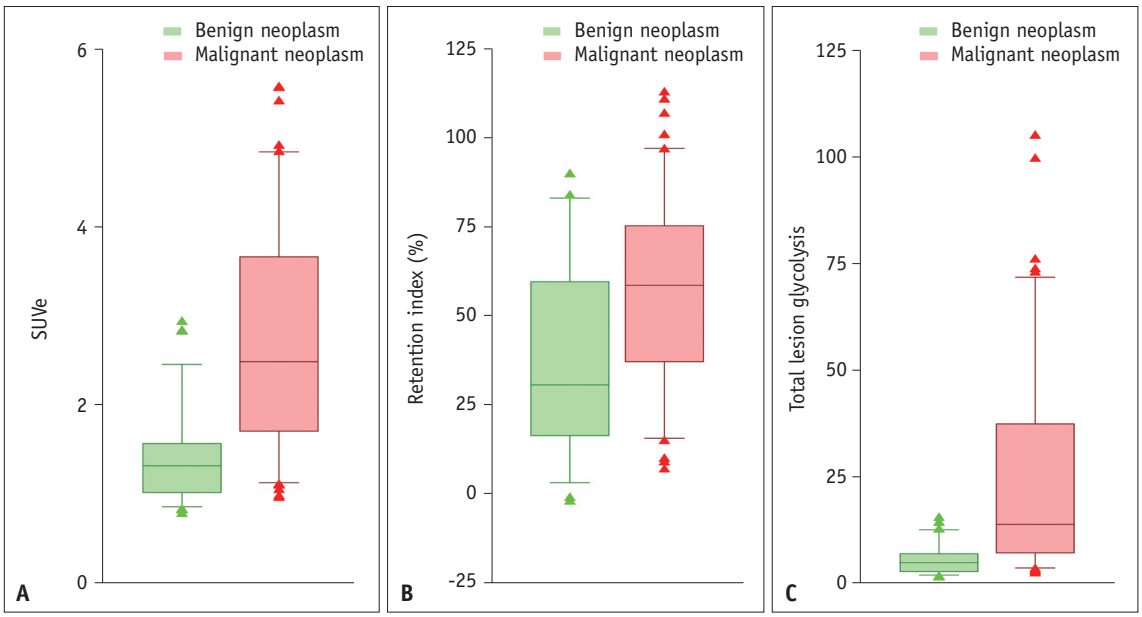

Fig. 3. Box plot comparisons of positron emission tomography parameters showed significant differences between benign and malignant pathology groups (**A-C**, $P < 0.001$). SUVe = blood-pool corrected peak standardized uptake value in early-phase scan

performances (Supplementary Tables 3, 4). A multimodal risk score was established according to the model's coefficient formula, as listed below and in Tables 4, 5.

1.6 x Jaundice + 1.9 x Malignant traits + 1.7 x SUVe ≥ 1.7 + 1.6 x PET-detected node

Combining Clinical Symptoms, Endoscopic Features, and PET Parameters to Predict the Risk of Ampullary Cancer

The multimodal risk score showed a sensitivity of 88.4% (95% CI, 79.7%–94.3%) and specificity of 77.8% (95% CI, 65.5%–87.3%) in predicting ampullary malignancy using a cut-off value of 3.3 (Table 5). ROC analysis highlighted superior diagnostic efficacy when incorporating PET parameters, outperforming endoscopy alone (AUC: 0.925 [95% CI, 0.874–0.956] vs. 0.815 [95% CI, 0.732–0.873], $P < 0.001$), and even endoscopy with jaundice (AUC: 0.925 [95% CI, 0.874–0.956] vs. 0.866 [95% CI, 0.796–0.913], $P < 0.001$, Table 5, Fig. 4A). Using the same cut-off, the model achieved a sensitivity of 88.0% (95% CI, 68.8%–97.5%), specificity of 75.6% (95% CI, 60.5%–87.1%), and AUC of 0.921 (95% CI, 0.816–0.967) in the EP candidates group, as shown in Figure 4B. Our model appropriately reassigned 7 (10%) of the 70 EP candidates to a more suitable resection method than endoscopy alone. Figure 5 illustrates a case that emphasizes the effectiveness of the model.

DISCUSSION

In this study, we investigated whether 2-[^{18}F]FDG PET/CT could help evaluate the risk of cancer in patients with endoscopy-detected ampullary neoplasms. We found that: 1) PET/CT can predict the risk of malignancy for endoscopy-detected ampullary tumors (OR, 16.06; $P < 0.001$), 2) jaundice, malignant traits in endoscopy, a hypermetabolic ampullary tumor, and PET-detected nodal disease were independent predictors of malignancy, 3) a risk model that incorporates these independent predictors outperforms endoscopy alone in predicting ampullary malignancy (AUC, 0.925 vs. 0.815, $P < 0.001$), 4) sensitivity analysis with an AUC of 0.921 affirmed the robustness of the risk model in EP candidates, 5) moreover, the risk model could potentially modify treatment strategy by 10.0% compared to relying solely on endoscopic diagnosis, highlights the importance of integrating 2-[^{18}F]FDG PET/CT in endoscopic treatment decisions.

This study found a significant correlation between hypermetabolic ampullary tumors detected by PET/CT and an increased malignancy risk. 2-[^{18}F]FDG PET/CT, a noninvasive tool for staging cancers with upregulated glucose metabolism, is widely used [17-19,24,34]. Watanabe et al. [25] highlighted the link between tumor SUVmax, tumor invasion extent, and nodal metastasis, potentially guiding the choice of EP over surgery in tumors with a low

https://doi.org/10.3348/kjr.2023.0295

Korean Journal of Radiology
KJR

Table 4. Univariable and multivariable analysis in predicting ampullary cancer

	Univariable		Multivariable	
	Unadjusted OR	*P*	Adjusted OR	*P*
Age, yrs (for increase by 1)	0.99 [0.96–1.01]	0.345		
Sex (male vs. female)*	0.96 [0.51–1.82]	0.901		
Overweight (BMI ≥ 25 vs. < 25 kg/m^2)*	0.51 [0.26–1.01]	0.054		
Diabetes (present vs. absent)*	1.11 [0.54–2.27]	0.783		
Dyslipidemia (present vs. absent)*	0.53 [0.21–1.36]	0.187		
Smoking (ever vs. never)*	1.46 [0.69–3.09]	0.321		
Drinking (ever vs. never)*	1.02 [0.42–2.49]	0.968		
Presenting symptoms*				
Pain (present vs. absent)	0.35 [0.18–0.67]	0.002	Eliminated	
Jaundice (present vs. absent)	7.53 [3.41–16.64]	< 0.001	4.89 [1.80–13.33]	0.002
Fever (present vs. absent)	2.90 [1.10–7.66]	0.032	Eliminated	
Elevated tumor markers*				
CA19-9 (≥ 37 vs. < 37 U/mL)	4.06 [1.92–8.59]	< 0.001	Eliminated	
CEA (≥ 5 vs. < 5 ng/mL)	2.80 [0.75–10.46]	0.127		
Endoscopy findings				
Malignant traits (present vs. absent)*	12.33 [5.52–27.56]	< 0.001	6.80 [2.41–19.20]	< 0.001
Size, mm (for increase by 1)	1.10 [1.04–1.16]	0.002	Eliminated	
Ductal dilatation (present vs. absent)*	4.26 [1.84–9.82]	0.001	Eliminated	
PET findings*				
Ampullary tumor				
Visual assessment (positive vs. negative)				
Early-phase	6.58 [3.13–13.82]	< 0.001	Multicollinearity	
Delayed-phase	9.63 [4.40–21.09]	< 0.001	Multicollinearity	
Semiquantitation				
SUVe (≥ 1.7 vs. < 1.7)	16.06 [7.13–36.18]	< 0.001	5.43 [2.00–14.72]	< 0.001
RI (≥ 35% vs. < 35%)	4.80 [2.37–9.75]	< 0.001	Eliminated	
TLG (≥ 7.0 vs. < 7.0)	11.60 [5.41–24.85]	< 0.001	Eliminated	
Positive node (present vs. absent)	14.58 [4.25–49.96]	< 0.001	5.03 [1.16–21.86]	0.041
Metastasis (present vs. absent)	14.85 [0.85–260.01]	0.065		

Coefficient formula: 1.6 x Jaundice + 1.9 x Malignant traits + 1.7 x SUVe ≥ 1.7 + 1.6 x PET-detected node.
*For categorical variables with categories in parentheses, the former was compared with the latter (the reference) to calculate ORs and 95% confidence intervals with the logistic regression analysis.
OR = odds ratio, BMI = body mass index, CA19-9 = carbohydrate antigen 19-9, CEA = carcinoembryonic antigen, PET = positron emission tomography, SUVe = blood-pool corrected peak standardized uptake value in early-phase scan, RI = retention index, TLG = total lesion glycolysis

Table 5. Diagnostic performance comparing endoscopy, endoscopy with jaundice, and the multimodal risk score (including PET parameters)

Modality	Endoscopy	Endoscopy + jaundice*	Multimodal risk score†
Sensitivity	86.1 (74/86) [76.9–92.6]	94.2 (81/86) [87.0–98.1]	88.4 (76/86) [79.7–94.3]
Specificity	66.7 (42/63) [53.7–78.1]	58.7 (37/63) [45.6–71.0]	77.8 (49/63) [65.5–87.3]
Positive predictive value	77.9 (74/95) [68.2–85.8]	75.7 (81/107) [66.5–83.5]	84.4 (76/90) [75.3–91.2]
Negative predictive value	77.8 (42/54) [64.4–88.0]	88.1 (37/42) [74.4–96.0]	83.1 (49/59) [71.0–91.6]
Area under the curve	0.815 [0.732–0.873]	0.866 [0.796–0.913]	0.925 [0.874–0.956]

Data are percentages with raw numbers in parentheses and 95% confidence interval values in brackets. Cut-offs for each model were determined using the Youden method.
*Endoscopy + jaundice = 1.6 x jaundice + 1.9 x malignant traits (cut-off value = 1.6), †Multimodal risk score = 1.6 x jaundice + 1.9 x malignant traits + 1.7 x SUVe ≥ 1.7 + 1.6 x PET-detected node (cut-off value = 3.3).
PET = positron emission tomography, SUVe = blood-pool corrected peak standardized uptake value in early-phase scan

https://doi.org/10.3348/kjr.2023.0295

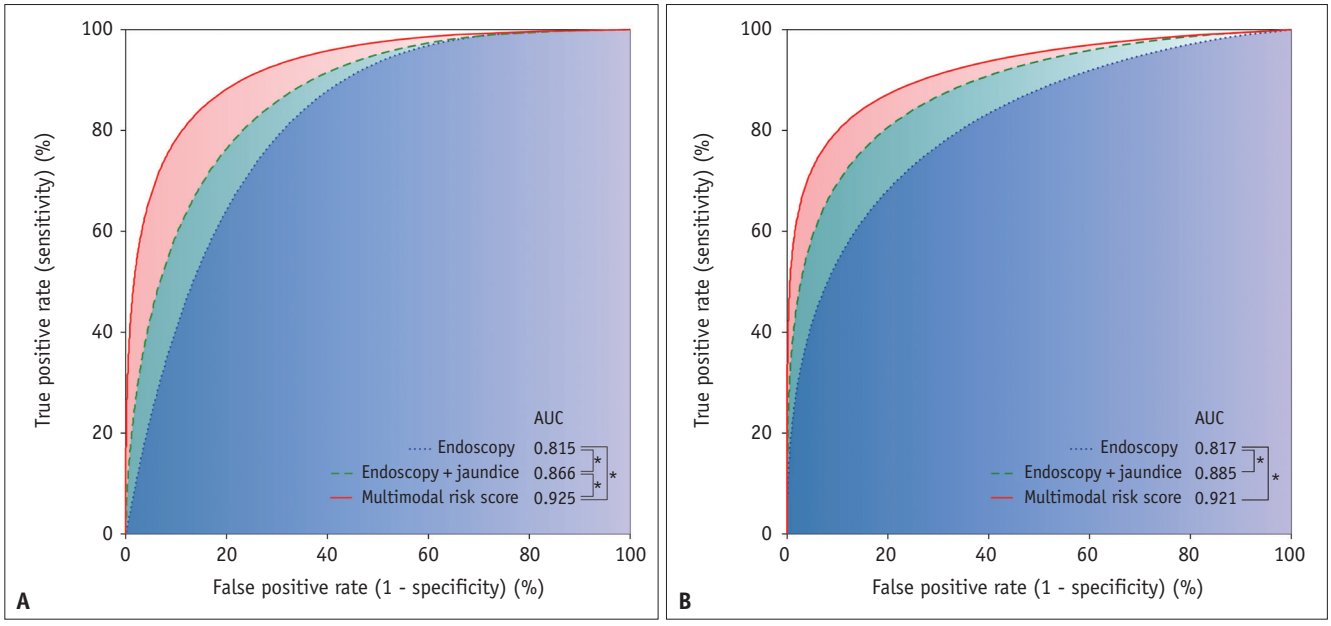

Fig. 4. Receiver operating characteristic curve analysis of the risk model in all the patients **(A)** and in subgroup analysis of candidates for endoscopic papillectomy **(B)**. Improved diagnostic performance was observed with additional clinical and positron emission tomography information compared to that of endoscopy alone. *P < 0.05. AUC = area under the curve

SUVmax. Consistent with this, our study noted that an SUVe ≥ 1.7 and PET-detected nodal disease are probable indicators of ampullary cancer. In line with these findings, Wen et al. [35] found that visually assessed 2-[^{18}F]FDG PET/CT had a higher specificity (78.6%) for differentiating between benign and malignant ampullary tumors than contrast-enhanced CT or magnetic resonance imaging (MRI) (35.7%), while maintaining a similar sensitivity of approximately 90%. They also noted greater diagnostic uncertainty in smaller tumors, especially those < 15 mm [35]. Using SUVpeak, a more robust and reproducible semiquantitative PET parameter [23,31,35], our results demonstrated good specificity of 82.8% in tumors sized 17.1 ± 7.7 mm using the dual-phase imaging [32,36]. Utilizing oral foaming contrast in our protocol enhanced the background-to-target contrast and improved tumor delineation, facilitating image interpretation [23]. Notably, all ampullary tumors in our cohort were detected using endoscopy, a clinical scenario frequently encountered in which a decision to perform EP, local resection, or pancreaticoduodenectomy must be made. The diagnostic performance of 2-[^{18}F]FDG PET/CT was not inferior to that of endoscopy in detecting ampullary cancer (accuracy, 79.4% vs. 75.5%).

In addition to ampullary lesions, PET-detected nodal disease was an independent predictor of malignancy in the present study. 2-[^{18}F]FDG PET/CT is also well-known for its ability to detect distant metastasis [23,35,37]. Metastatic foci revealed by PET/CT displayed 100% specificity and PPV for malignancy. Our cohort, using 2-[^{18}F]FDG PET/CT for N staging, showed superior sensitivity (54.3%) compared with the 25.0% reported by Chen et al. [38] using MRI. As highlighted in our previous studies, PET-derived N and M stages offer prognostic insights for patients with ampullary cancer, underscoring the potential of 2-[^{18}F]FDG PET/CT in treatment planning [23,35,37].

Clinical information is equally important in diagnosing ampullary cancers [3,6]. In our analysis, jaundice independently predicted malignancy and was included in the risk model. Despite its reported utility in detecting nodes in periampullary cancers, elevated serum CA19-9 levels could not reliably distinguish malignant from benign tumors, possibly because of the high cholangitis and ductal dilation rates in our cohort [39,40]. Applying a 37 U/mL cut-off, patients with higher CA19-9 levels had a 4.1-fold higher risk of malignancy (P < 0.001). However, this significance was diminished in multivariable and subgroup analyses, indicating a diminished role of traditional biochemical markers in differentiating early small cancers from adenomas [41]. Interestingly, a borderline association was observed between non-overweight status and cancer, particularly among EP candidates. One possible explanation may be cancer-associated mass wasting [42]; however, further

https://doi.org/10.3348/kjr.2023.0295

Korean Journal of Radiology
KJR

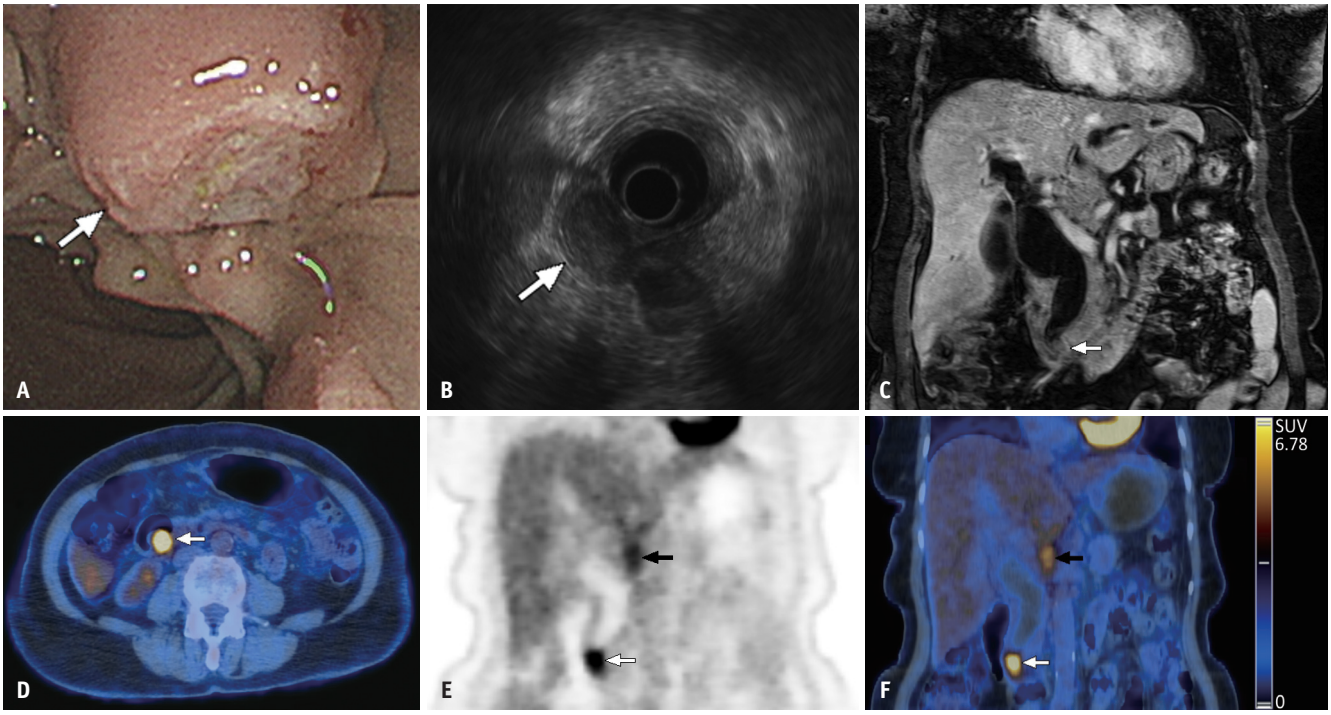

Fig. 5. A 70-year-old female with a painful biliary obstruction was found to have an elevated CA19-9 level (51.6 U/mL). **A-F:** Endoscopy identified villous mucosal change of the ampulla without ulceration, bleeding, or friability (arrow, **A**). Endoscopic ultrasonography revealed a 16.6 mm hypoechoic tumor limited to the ampulla (arrow, **B**). There was no submucosal invasion or intraductal growth. The biopsy revealed a high-grade dysplastic neoplasm. Magnetic resonance imaging showed insignificant change of the ampulla (arrow, **C**) despite a marked dilated bile duct. 2-[18F]FDG PET/CT revealed a hypermetabolic ampulla with an SUVe of 3.2, retention index of 34%, and total lesion glycolysis of 23.5 (white arrows, **D, E, F**). The ampulla of Vater was clearly delineated using oral contrast (arrow, **D**). A few positive nodes near the hepatic artery were also visualized (black arrows, **E, F**). The patient was considered to have a low risk of cancer according to endoscopy and clinical presentation and was considered to be eligible for endoscopic papillectomy. However, a multimodal risk score of 4.9 was obtained after combining 2-[18F]FDG PET/CT information, indicating a high risk of occult malignancy. She received pancreaticoduodenectomy, and the final diagnosis showed adenocarcinoma of intestinal type. CA19-9 = carbohydrate antigen 19-9, 2-[18F]FDG PET/CT = 2-[18F]fluoro-2-deoxy-D-glucose positron emission tomography/computed tomography, SUVe = blood-pool corrected peak standardized uptake value in early-phase scan

information is needed to validate this hypothesis.

This single-center cohort study has some limitations. First, referral bias was inevitable, as the patients were referred for additional 2-[18F]FDG PET/CT only when decisions were difficult, resulting in a higher prevalence of N1 disease in our cohort [2-4]. This could be explained by the rarity of ampullary tumors [2]. Our results emphasize the use of 2-[18F]FDG PET/CT as an advanced imaging technique in real-world practice. Second, post-procedural inflammation could potentially affect 2-[18F]FDG PET/CT interpretation, leading to false positives [16]. However, owing to the necessity of prompt intervention in cases of tumor-related obstruction [3,4,12], delaying imaging and treatment is not ethical. Moreover, our study demonstrated the utility of PET/CT in assessing the malignancy risk in ampullary tumors, even when performed just 5 days after endoscopy or biliary drainage. Third, the risk model was not validated externally. Potential confirmation bias implies that our results should be interpreted with caution when applied to EP candidates. Finally, the lack of head-to-head comparisons among 2-[18F]FDG PET/CT, contrast-enhanced CT, and MRI may have limited the utility of PET/CT in the differential diagnosis of ampullary tumors in real-world scenarios, particularly for patients who contemplating surgical resection. More patients should be enrolled in future multicenter studies to validate the results of our study and their impact on treatment planning.

In conclusion, we demonstrated that a multimodal approach combining clinical data, endoscopy, and 2-[18F]FDG PET/CT improved the assessment of the malignancy risk in patients with endoscopy-detected ampullary tumors. This may help refine therapeutic decision-making, particularly when considering EP as a surgical alternative.

https://doi.org/10.3348/kjr.2023.0295

Supplement

The Supplement is available with this article at https://doi.org/10.3348/kjr.2023.0295.

Availability of Data and Material

The datasets generated during and/or analyzed during the current study are available from the corresponding author on reasonable request.

Conflicts of Interest

The authors have no potential conflicts of interest to disclose.

Author Contributions

Conceptualization: Hsiu-Po Wang, Mei-Fang Cheng. Data curation: Pei-Ju Chuang, Mei-Fang Cheng. Formal analysis: Pei-Ju Chuang, Wei-Shan Chin. Funding acquisition: Yu-Wen Tien, Mei-Fang Cheng. Investigation: Hsiu-Po Wang, Yu-Wen Tien, Min-Shu Hsieh, Chieh-Chang Chen, Tzu-Chan Hong. Methodology: Hsiu-Po Wang, Yu-Wen Tien, Yen-Wen Wu, Mei-Fang Cheng. Project administration: Hsiu-Po Wang, Yu-Wen Tien, Mei-Fang Cheng. Resources: Yu-Wen Tien, Mei-Fang Cheng. Software: Pei-Ju Chuang, Chi-Lun Ko, Yen-Wen Wu, Mei-Fang Cheng. Supervision: Hsiu-Po Wang, Yu-Wen Tien, Yen-Wen Wu, Mei-Fang Cheng. Validation: Wei-Shan Chin, Mei-Fang Cheng. Visualization: Pei-Ju Chuang, Chi-Lun Ko. Writing—original draft: Pei-Ju Chuang. Writing—review & editing: Tzu-Chan Hong, Mei-Fang Cheng.

ORCID IDs

Pei-Ju Chuang
https://orcid.org/0000-0002-3613-2756
Hsiu-Po Wang
https://orcid.org/0000-0002-7741-9315
Yu-Wen Tien
https://orcid.org/0000-0002-9126-2705
Wei-Shan Chin
https://orcid.org/0000-0001-9295-7966
Min-Shu Hsieh
https://orcid.org/0000-0002-0594-3732
Chieh-Chang Chen
https://orcid.org/0000-0003-2953-210X
Tzu-Chan Hong
https://orcid.org/0000-0003-2475-3835
Chi-Lun Ko
https://orcid.org/0000-0002-4139-5892
Yen-Wen Wu
https://orcid.org/0000-0003-1520-1166
Mei-Fang Cheng
https://orcid.org/0000-0002-9359-0606

Funding Statement

This work was partly supported by the Ministry of Science and Technology of Taiwan (MOST 112-2314-B-002-251-) to the author MF Cheng and YW Tien; and the National Taiwan University Hospital (NTUH-97N-1008, NTUH-100-N1732, and NTUH-103-S2397) to the author MF Cheng. The funding source has no role in the design, practice or analysis of this study. All other authors declare that they have no competing interests.

Acknowledgments

The authors thank the Center of Statistical Consultation and Research in the Department of Medical Research for statistical assistance, and all colleagues in the Nuclear Medicine Department for image acquisition and processing. The authors also thank the National Taiwan University Hospital and National Taiwan University College of Medicine for their generous support.

REFERENCES

1. Campbell DR Jr, Lee JH. A comprehensive approach to the management of benign and malignant ampullary lesions: management in hereditary and sporadic settings. *Curr Gastroenterol Rep* 2020;22:46
2. Ramai D, Ofosu A, Singh J, John F, Reddy M, Adler DG. Demographics, tumor characteristics, treatment, and clinical outcomes of patients with ampullary cancer: a surveillance, epidemiology, and end results (SEER) cohort study. *Minerva Gastroenterol Dietol* 2019;65:85-90
3. Vanbiervliet G, Strijker M, Arvanitakis M, Aelvoet A, Arnelo U, Beyna T, et al. Endoscopic management of ampullary tumors: European Society of Gastrointestinal Endoscopy (ESGE) guideline. *Endoscopy* 2021;53:429-448
4. Itoi T, Ryozawa S, Katanuma A, Kawashima H, Iwasaki E, Hashimoto S, et al. Clinical practice guidelines for endoscopic papillectomy. *Dig Endosc* 2022;34:394-411
5. Panzeri F, Crippa S, Castelli P, Aleotti F, Pucci A, Partelli S, et al. Management of ampullary neoplasms: a tailored approach between endoscopy and surgery. *World J Gastroenterol* 2015;21:7970-7987
6. Ardengh JC, Kemp R, Lima-Filho ÉR, Dos Santos JS. Endoscopic papillectomy: the limits of the indication, technique and results. *World J Gastrointest Endosc* 2015;7:987-994
7. Moon JH, Choi HJ, Lee YN. Current status of endoscopic

papillectomy for ampullary tumors. *Gut Liver* 2014;8:598-604
8. Yamamoto K, Iwasaki E, Itoi T. Insights and updates on endoscopic papillectomy. *Expert Rev Gastroenterol Hepatol* 2020;14:435-444
9. Sahar N, Krishnamoorthi R, Kozarek RA, Gluck M, Larsen M, Ross AS, et al. Long-term outcomes of endoscopic papillectomy for ampullary adenomas. *Dig Dis Sci* 2020;65:260-268
10. Spadaccini M, Fugazza A, Frazzoni L, Leo MD, Auriemma F, Carrara S, et al. Endoscopic papillectomy for neoplastic ampullary lesions: a systematic review with pooled analysis. *United European Gastroenterol J* 2020;8:44-51
11. Winter JM, Cameron JL, Olino K, Herman JM, de Jong MC, Hruban RH, et al. Clinicopathologic analysis of ampullary neoplasms in 450 patients: implications for surgical strategy and long-term prognosis. *J Gastrointest Surg* 2010;14:379-387
12. ASGE Standards of Practice Committee; Chathadi KV, Khashab MA, Acosta RD, Chandrasekhara V, Eloubeidi MA, Faulx AL, et al. The role of endoscopy in ampullary and duodenal adenomas. *Gastrointest Endosc* 2015;82:773-781
13. Angthong W, Jiarakoop K, Tangtiang K. Differentiation of benign and malignant ampullary obstruction by multi-row detector CT. *Jpn J Radiol* 2018;36:477-488
14. Artifon EL, Couto D Jr, Sakai P, da Silveira EB. Prospective evaluation of EUS versus CT scan for staging of ampullary cancer. *Gastrointest Endosc* 2009;70:290-296
15. Cannon ME, Carpenter SL, Elta GH, Nostrant TT, Kochman ML, Ginsberg GG, et al. EUS compared with CT, magnetic resonance imaging, and angiography and the influence of biliary stenting on staging accuracy of ampullary neoplasms. *Gastrointest Endosc* 1999;50:27-33
16. Boellaard R, Delgado-Bolton R, Oyen WJ, Giammarile F, Tatsch K, Eschner W, et al. FDG PET/CT: EANM procedure guidelines for tumour imaging: version 2.0. *Eur J Nucl Med Mol Imaging* 2015;42:328-354
17. Mohamadien NRA, Sayed MHM. Correlation between semiquantitative and volumetric 18F-FDG PET/computed tomography parameters and Ki-67 expression in breast cancer. *Nucl Med Commun* 2021;42:656-664
18. Brito AF, Abrantes AM, Ribeiro M, Oliveira R, Casalta-Lopes J, Gonçalves AC, et al. Fluorine-18 fluorodeoxyglucose uptake in hepatocellular carcinoma: correlation with glucose transporters and p53 expression. *J Clin Exp Hepatol* 2015;5:183-189
19. Iwamoto M, Kawada K, Nakamoto Y, Itatani Y, Inamoto S, Toda K, et al. Regulation of 18F-FDG accumulation in colorectal cancer cells with mutated KRAS. *J Nucl Med* 2014;55:2038-2044
20. Kim BJ, Jang HJ, Kim JH, Kim HS, Lee J. KRAS mutation as a prognostic factor in ampullary adenocarcinoma: a meta-analysis and review. *Oncotarget* 2016;7:58001-58006
21. Kubota K, Fujita Y, Sato T, Watanabe S, Hosono K, Yoneda M, et al. Tumor diameter and Ki-67 expression in biopsy could be diagnostic markers discriminating from adenoma and early stage cancer in patients with ampullary tumors. *J Hepatobiliary Pancreat Sci* 2013;20:531-537
22. Chakraborty S, Ecker BL, Seier K, Aveson VG, Balachandran VP, Drebin JA, et al. Genome-derived classification signature for ampullary adenocarcinoma to improve clinical cancer care. *Clin Cancer Res* 2021;27:5891-5899
23. Chuang PJ, Wang HP, Lin YJ, Chen CC, Tien YW, Hsieh MS, et al. Preoperative 2-[18F]FDG PET-CT aids in the prognostic stratification for patients with primary ampullary carcinoma. *Eur Radiol* 2021;31:8040-8049
24. Park YM, Seo HI. Predictive value of metabolic activity detected by pre-operative 18F FDG PET/CT in ampullary adenocarcinoma. *Medicine (Baltimore)* 2021;100:e27561
25. Watanabe A, Harimoto N, Araki K, Kubo N, Igarashi T, Tsukagoshi M, et al. FDG-PET for preoperative evaluation of tumor invasion in ampullary cancer: a retrospective analysis. *J Surg Oncol* 2021;124:317-323
26. Jamar F, Buscombe J, Chiti A, Christian PE, Delbeke D, Donohoe KJ, et al. EANM/SNMMI guideline for 18F-FDG use in inflammation and infection. *J Nucl Med* 2013;54:647-658
27. Cheng MF, Wang HP, Tien YW, Liu KL, Yen RF, Tzen KY, et al. Usefulness of PET/CT for the differentiation and characterization of periampullary lesions. *Clin Nucl Med* 2013;38:703-708
28. Lasnon C, Desmonts C, Quak E, Gervais R, Do P, Dubos-Arvis C, et al. Harmonizing SUVs in multicentre trials when using different generation PET systems: prospective validation in non-small cell lung cancer patients. *Eur J Nucl Med Mol Imaging* 2013;40:985-996
29. Sunderland JJ, Christian PE. Quantitative PET/CT scanner performance characterization based upon the society of nuclear medicine and molecular imaging clinical trials network oncology clinical simulator phantom. *J Nucl Med* 2015;56:145-152
30. Koppula BR, Fine GC, Salem AE, Covington MF, Wiggins RH, Hoffman JM, et al. PET-CT in clinical adult oncology: III. Gastrointestinal malignancies. *Cancers (Basel)* 2022;14:2668
31. Sher A, Lacoeuille F, Fosse P, Vervueren L, Cahouet-Vannier A, Dabli D, et al. For avid glucose tumors, the SUV peak is the most reliable parameter for [(18)F]FDG-PET/CT quantification, regardless of acquisition time. *EJNMMI Res* 2016;6:21
32. Jia G, Zhang J, Li R, Yan J, Zuo C. The exploration of quantitative intra-tumoral metabolic heterogeneity in dual-time 18F-FDG PET/CT of pancreatic cancer. *Abdom Radiol (NY)* 2021;46:4218-4225
33. Unal I. Defining an optimal cut-point value in ROC analysis: an alternative approach. *Comput Math Methods Med* 2017;2017:3762651
34. Choi HJ, Kang CM, Jo K, Lee WJ, Lee JH, Ryu YH, et al. Prognostic significance of standardized uptake value on preoperative 18F-FDG PET/CT in patients with ampullary adenocarcinoma. *Eur J Nucl Med Mol Imaging* 2015;42:841-847
35. Wen G, Gu J, Zhou W, Wang L, Tian Y, Dong Y, et al. Benefits of 18F-FDG PET/CT for the preoperative characterisation or staging of disease in the ampullary and duodenal papillary.

Eur Radiol 2020;30:5089-5098
36. Kawada N, Uehara H, Hosoki T, Takami M, Shiroeda H, Arisawa T, et al. Usefulness of dual-phase 18F-FDG PET/CT for diagnosing small pancreatic tumors. *Pancreas* 2015;44:655-659
37. Raj P, Kaman L, Singh R, Dahyia D, Bhattacharya A, Bal A. Sensitivity and specificity of FDG PET-CT scan in detecting lymph node metastasis in operable periampullary tumours in correlation with the final histopathology after curative surgery. *Updates Surg* 2013;65:103-107
38. Chen CH, Yang CC, Yeh YH, Chou DA, Nien CK. Reappraisal of endosonography of ampullary tumors: correlation with transabdominal sonography, CT, and MRI. *J Clin Ultrasound* 2009;37:18-25
39. Alexakis N, Gomatos IP, Sbarounis S, Toutouzas K, Katsaragakis S, Zografos G, et al. High serum CA 19-9 but not tumor size should select patients for staging laparoscopy in radiological resectable pancreas head and peri-ampullary cancer. *Eur J Surg Oncol* 2015;41:265-269
40. Lin MS, Huang JX, Yu H. Elevated serum level of carbohydrate antigen 19-9 in benign biliary stricture diseases can reduce its value as a tumor marker. *Int J Clin Exp Med* 2014;7:744-750
41. Jin X, Wu Y. Diagnostic utility of clinical and biochemical parameters in pancreatic head malignancy patients with normal carbohydrate antigen 19-9 levels. *Afr Health Sci* 2015;15:123-130
42. Shi X, Yang J, Liu M, Zhang Y, Zhou Z, Luo W, et al. Circular RNA ANAPC7 inhibits tumor growth and muscle wasting via PHLPP2-AKT-TGF-β signaling axis in pancreatic cancer. *Gastroenterology* 2022;162:2004-2017.e2

https://doi.org/10.3348/kjr.2023.0295